Effect of Location Accuracy and Shadowing on the Probability of Non-Interfering Concurrent Transmissions in Cognitive Ad Hoc Networks

Samuel MONTEJO[1], *Richard Demo SOUZA*[2], *Evelio M. G. FERNANDEZ*[3], *Vitalio ALFONSO*[1], *Walter GODOY*[2]

[1]Dept. of Telecommunications, Central University of Las Villas, Santa Clara, Cuba
[2]CPGEI, Federal University of Technology - Paraná, Curitiba, Brazil
[3]Dept. of Electrical Engineering, Federal University of Paraná, Curitiba, Brazil

montejo@uclv.edu.cu, richard@utfpr.edu.br, evelio@ufpr.br, vitalio@uclv.edu.cu, godoy@utfpr.edu.br

Abstract. *Cognitive radio ad hoc systems can coexist with a primary network in a scanning-free region, which can be dimensioned by location awareness. This coexistence of networks improves system throughput and increases the efficiency of radio spectrum utilization. However, the location accuracy of real positioning systems affects the right dimensioning of the concurrent transmission region. Moreover, an ad hoc connection may not be able to coexist with the primary link due to the shadowing effect. In this paper we investigate the impact of location accuracy on the concurrent transmission probability and analyze the reliability of concurrent transmissions when shadowing is taken into account. A new analytical model is proposed, which allows to estimate the resulting secure region when the localization uncertainty range is known. Computer simulations show the dependency between the location accuracy and the performance of the proposed topology, as well as the reliability of the resulting secure region.*

Keywords

Cognitive radio, concurrent transmissions, location accuracy, location awareness.

1. Introduction

The inefficient use of the radio spectrum imposes the utilization of a communication technology that allows its exploitation in a more intelligent and flexible way [1]. The literature provides evidence of the inefficiency of conventional fixed spectrum allocation [2–5]. For these reasons, the Federal Communications Commission (FCC) has considered a more flexible, efficient, and comprehensive use of the available spectrum through cognitive radio (CR) [6]. Originally proposed in [7], CR is a key technology to solve this problem by allowing opportunistic spectrum access, ensuring the exploitation of underutilized bands and thus increasing the efficiency of spectrum use.

In CR networks the cognitive (secondary) users attempt to operate on the same frequency band of licensed (primary) users. Therefore, an important tradeoff between protecting the primary network communication and maximizing the throughput of the secondary network is established, which depends on the temporal and spatial holes detected in the frequency band. Excellent studies related to CR systems are provided in [1, 8–10].

In [11], the FCC recognizes three methods that could assist CR devices to determine whether a portion of the frequency spectrum is unused at a specific time and/or location: control signal beacons, spectrum sensing and location awareness. The first method minimizes the risk for primary users of being interfered by unlicensed users since they are not allowed to access the communication channel unless the legacy system explicitly permits it. The major drawback of this scheme is that it requires the establishment of an expensive infrastructure which makes it impractical in most cases. Spectrum sensing has attracted a great deal of attention because of its broader application areas and lower infrastructure requirements. Using this method unlicensed transmitters listen to the frequency spectrum in order to detect if other transmitters are operating in the area.

A complete review of spectrum sensing algorithms can be found in [9, 12, 13]. Furthermore, a power allocation scheme is presented in [14] to provide optimal energy-efficient normalized throughput in cognitive relay networks, where the authors jointly consider the transmit rate and power consumption. In [15] the power allocation and beamforming is investigated in a relay assisted cognitive radio network, to maximize the performance of the CR network while limiting interference in the direction of the primary users. The proposed approach employs genetic algorithm to solve the optimization problems. In [16], it is addressed a power and subcarrier allocation scheme for cooperative cognitive radio networks in the presence of spectrum sens-

ing errors. However, CR devices are expected to perform extensive search in wide spectrum areas, representing a heavy hardware, time, energy and memory consuming task [17,18].

Location awareness has been proposed to assist the spectrum management and other areas related to CR such as location based services [19, 20]. Location information has been commonly used in traditional wireless networks to assist applications and services such as emergency calls, fraud detection and vehicular traffic management [21]. Recently, Gorcin [22] has shown the importance of the integration of location awareness with cognitive radio in public safety communications in order to identify opportunities for frequency spectrum reuse, which is the main and most distinctive property in cognitive radio. Exhaustive comparisons between geolocation techniques and spectrum sensing can be found in [23, 24].

In a scenario where the CR users are sufficiently far from the primary users it is possible to transmit concurrently without secondary and primary users interfering with each other. In order to avoid the high implementation complexity, the excessive consumption of time and energy, as well as the nonzero probability of false detection related to spectrum sensing techniques, in [17, 25–31] sensing-free spectrum sharing scenarios were addressed. These scenarios aimed to establish an ad-hoc overlaying network on top of an infrastructure-based legacy network. Therefore, if location awareness capability of the CR devices is enabled, then the dimensioning of a scanning-free or concurrent transmission region ($\mathcal{R}_{CT}$) is possible. This overlapping between cognitive and ad hoc networks increases the overall system throughput by identifying and exploiting spatial spectrum holes.

The coexistence issue of the hybrid infrastructure-based and overlaying ad hoc networks has been addressed, but in different scenarios. In [32–35], this idea was proposed to extend the coverage area of the infrastructure-based network. The coverage area of ad hoc networks is not overlapped with that of the infrastructure-based network. In [36], as to further improve the throughput of a wireless local area network (WLAN), it was suggested that an access point (AP) could be dynamically switched between the infrastructure mode and the ad hoc mode whereas in [37] the issue of maximizing the number os secondary users is addressed. In our proposal, the decision of establishing ad hoc connections is made by the CR users in an autonomous and distributed way, which is a more flexible strategy.

In [25] a concurrent transmission region was dimensioned from a geometric point of view, considering primary and secondary transmit powers as fixed and equal. This approach has been the starting point of several researches [17, 27–31], where the CR users must be perfectly aware of their locations, as well as those of other mobile stations (MS) in the primary network. In [27] the impact of channel rate control on the performance of a cognitive radio ad hoc network overlaying an infrastructure-based system was investigated. The proposed algorithm properly adjusts the secondary users rate to be as large as possible by increasing their average rate, without affecting the primary users. In [17] an algorithm for optimal power control was proposed to maximize the scanning-free region, whose trivial circular shape was possible due to the lower transmission power of secondary devices compared to the one used in the primary network. In [28] the impact of power control on the concurrent transmission probability was studied, and a new analytical model was proposed to estimate the resulting expanded region when power adjustment is made between known limits. In [29] the impact of joint rate and power control on the performance of a cognitive radio ad hoc network overlaying a primary system was considered. Two power control strategies were proposed: RE-PC to maximize the secondary capacity, and EE-PC to minimize the secondary energy consumption. On the other hand, in [30] a dynamic spectrum sharing method was proposed which allows multiple secondary users to reside in the same channel and use it concurrently exploiting variable transmission power and location information. Finally, the benefits that power control and antenna directivity can bring to the total sum rate of a multiuser cognitive radio network were analyzed in [31]. However, it should be noted that these studies did not consider the location accuracy. The impact of such an important parameter has been subject of several investigations [21, 22, 38–46]. The computation of theoretical limits for positioning accuracy presented in [21,44,45] shows the non-existence of systems with absolute accuracy.

Then, the main objective of this paper is to identify and discuss the impact of location accuracy on the concurrent transmission region and on the coexistence probability of the primary and secondary networks. The area of this region (which will be called the *secure concurrent transmission region*, $\mathcal{R}_{CTS}$) is delimited considering the location uncertainty of mobile devices. A condensed, preliminary version of this result was presented in [47]. In addition, the reliability of the system according to the resulting secure region, when the effect of shadowing is taken into account, is now investigated.

The remainder of this paper is organized as follows. In Section II, the system model and problem formulation are presented. In Section III the uplink analysis in ideal and real conditions is addressed while shadowing effects are considered in Section IV. In Section V numerical results are presented. Finally, Section VI concludes the paper.

2. System Model and Problem Formulation

In this section a spectrum sharing scenario is considered in which a cognitive radio ad hoc network (CRAHN) operates inside the licensed network coverage area. Figure 1 shows the system model, which consists of one cognitive radio transmitter (CTx), one cognitive radio receiver (CRx),

one primary transmitter (PMS: Primary Mobile Station) and one primary receiver (BS: Base Station). The system is assumed to be interference limited. Moreover, for reasons of conciseness and clarity, the following approach focuses only on the uplink of the primary network. However, the model and ideas described in this paper can also be easily adapted and applied to the downlink.

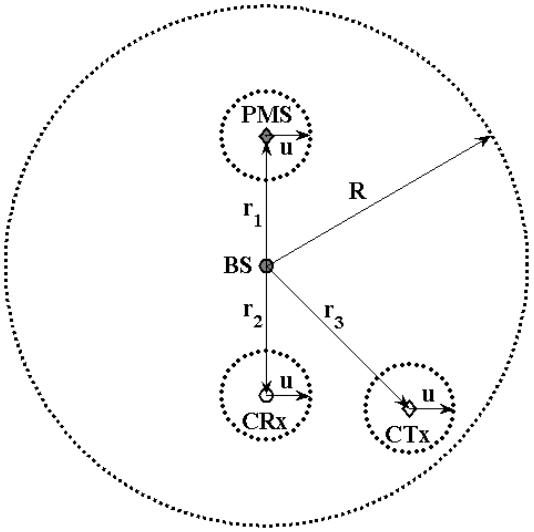

Fig. 1. A spectrum sharing scenario between a CRAHN and an infrastructure-based network, in which location uncertainty is represented by *uncertainty circles* of radius u centered at the detected positions of the the mobile devices.

It is considered that the CR devices can be assisted by positioning techniques in order to know their relative or absolute locations, as well as those of the PMSs; either through GPS or other positioning methods like those described in [41–43, 48, 49]. Moreover, the location information can be broadcasted by using geographical routing protocols [50, 54]. Despite the fact that these tasks consume time, memory and energy, the consumption of these resources is in general smaller than it would be if spectrum sensing was used, since the position estimation is only necessary when a new node joins the network or when a node changes its position.

In this scenario, the secondary users attempt to establish peer-to-peer connections, under the premise of not interfering the primary users. Without loss of generality, we assume that the BS is at the origin of coordinates and the mobile devices locations are represented by their polar coordinates as: (r_i, θ_i), $i = 1, 2, 3$, representing the PMS, the CRx and the CTx, respectively, within the coverage area of the BS (πR^2). Moreover, the index $i = 0$ is reserved to the BS. Each device is represented at the location detected by the positioning system. In addition, it is denoted by u the radius of the uncertainty circle associated with each mobile device, so that πu^2 is the area of the region where the device is certainly located. There are the several factors which can cause the uncertainty to vary between different devices such as the number of available reference nodes or environment obstacles which cause NLOS errors on some devices. However, for simplicity in this paper the accuracy is not considered as a function of a particular node and therefore the maximum error (u) for all nodes locations are assumed to be equal.

The goal is to dimension a secure concurrent transmission region that ensures non-interference between primary and secondary users, despite the location inaccuracies. Our approach takes as starting point the scenario presented in [25] and then analyzes the effect of the location uncertainty and shadowing. In order to characterize the quality of the links, two values of signal-to-interference ratio (SIR) are used: SIR_p, perceived by the BS and referred to the primary link (infrastructure-based network) and SIR_s, perceived by the CRx and referred to the secondary link (ad hoc network). The SIR thresholds required for successful reception at the primary and secondary networks are denoted by τ_p and τ_s, respectively. The region where both thresholds are exceeded is the concurrent transmission region.

Then, the probability of existence of an interference-free concurrent transmission is:

$$\mathcal{P}_{CT} = \mathcal{P}\{(SIR_p > \tau_p) \cap (SIR_s > \tau_s)\} \tag{1}$$

where $\mathcal{P}\{\phi\}$ is the probability of event ϕ. The calculation of this parameter represents an important step in order to decide whether to reuse the selected frequency band (by means of concurrent transmissions) or to select another frequency band for the cognitive devices.

Moreover, based on a log-distance propagation model [55], the received power at a given node can be written as:

$$P_r = \frac{P_t \kappa 10^{(\varepsilon/10)}}{d_{tr}^{\alpha}} \tag{2}$$

where P_r and P_t represent the received and transmitted power levels, respectively, κ is a factor taking into account the antenna heights and antenna gains (for the sake of simplicity we consider $\kappa = 1$ in this paper), d_{tr} is the distance between the transmitter and receiver, α is the path loss exponent, and $10^{(\varepsilon/10)}$ is the log-normal distributed shadowing component.

3. Uplink Signal to Interference Rate Analysis

3.1 Ideal Conditions

First, an ideal scenario is considered in which the location uncertainty and the shadowing effect are not taken into account. The primary and secondary transmission powers are considered to be equal, as in [25]. Thus, due to the similar interference ranges, it is reasonable to assume that only a couple of secondary devices may establish a link at a time.

Let P_{10} and P_{30} be the received power from the PMS and CTx at the BS, respectively. Similarly, P_{32} and P_{12} represent the received power from the CTx and PMS at the CRx,

respectively. As in this case we consider that there is no uncertainty regarding the detected positions of the mobile devices, the signal-to-interference ratio in each link can be represented as:

$$SIR_p = \frac{P_{10}}{P_{30}} = \left(\frac{r_3}{r_1}\right)^{\alpha}, \tag{3}$$

$$SIR_s = \frac{P_{32}}{P_{12}} = \left(\frac{d_{12}}{d_{32}}\right)^{\alpha} \tag{4}$$

where d_{12} and d_{23} are the distances from PMS and CTx to the CRx, respectively. If the devices locations are known, these distances can be computed as: $d_{ij} = \sqrt{r_i^2 + r_j^2 - 2r_i r_j \cos(\theta_i - \theta_j)}$. Then, substituting (3) and (4) into (1), the concurrent transmission probability becomes:

$$\mathcal{P}_{CT} = \mathcal{P}\left\{\left(r_1\tau_p^{1/\alpha} < r_3 < R\right) \cap \left(d_{32} < \frac{d_{12}}{\tau_s^{1/\alpha}}\right)\right\} \triangleq \frac{\mathcal{R}_{CT}}{\pi R^2}. \tag{5}$$

Note that $\mathcal{R}_{CT}$ is the area of the region where the CTx can successfully communicate with the CRx without interfering the primary link.

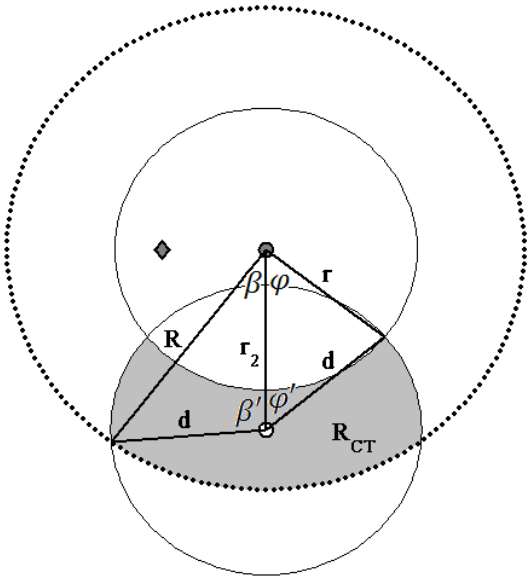

Fig. 2. Concurrent transmission region considering the detected positions as absolutely accurate. The PMS is located at $(40\,\text{m}, \pi)$ and the CRx is located at $\left(75\,\text{m}, \frac{3\pi}{2}\right)$.

The first boundary condition $r_1\tau_p^{1/\alpha} < r_3 < R$, represents the proximity limit between the CTx and the BS, which guarantees the primary link quality, ensuring that $SIR_p > \tau_p$. This protection radius is denoted as r in Fig. 2 and the circular region of radius r centered at the BS is defined as the *forbidden region*. The requirement $r_3 < R$ limits the location of the CTx within the BS coverage area. Finally, $d_{32} < \frac{d_{12}}{\tau_s^{1/\alpha}}$ indicates the maximum separation between the CRx and the CTx, which guarantees the secondary link quality, ensuring that $SIR_s > \tau_s$. This distance is denoted as d in Fig. 2 and the circular region of radius d centered at the detected position of the CRx is defined as the *effective cognitive region*.

Then, the concurrent transmission region is defined as the intersection between the circle of radius d and the ring delimited by r and R. This region is shadowed in Fig. 2 and its area is given by:

$$\mathcal{R}_{CT} = \pi d^2 - A_1 - A_2 \tag{6}$$

where

$$A_1 = (\pi - \beta')d^2 - \beta R^2 + 2A_3, \tag{7}$$

and

$$A_2 = \varphi' d^2 + \varphi r^2 - 2A_4 \tag{8}$$

where A_3 represents the area of the triangle formed by R, r_2 and d, and A_4 is the area of the triangle formed by r, r_2 and d. Knowing the side lengths, both areas can be calculated by Heron's formula. Similarly, the angles involved (which are also shown in Fig. 2) can be found through the law of cosines.

A similar approach is presented in [25]. However, this is a very optimistic approach, as it considers that the measured mobile station location is absolutely accurate. In the next section we address the practical case of positioning system accuracy.

3.2 Real Conditions

Taking location uncertainty into account means that we cannot rely on the exact coordinates obtained from the positioning system. We can only trust that the i-th mobile station (MS_i) is located in a region centered at (r_i, θ_i) with radius u, according to the positioning system accuracy.

This region depends on the area of the ring defined by R and r, and on the area of the circle of radius d. The magnitude of the radius R depends on the transmitted power at the BS, whose location is considered to be fixed and known. In contrast, r does not only depend on α and τ_p, but also on r_1, which does depend on the PMS location and hence on the positioning system accuracy. Moreover, d depends on the distance from the CRx to the PMS, therefore on their locations as well.

In order to find the secure transmission region we need to consider the most stringent boundary conditions for any possible combination of the CRx and PMS locations. What most affects the area of the ring is increasing r, so the worst case is when the PMS is located at the farthest point from the BS, inside the uncertainty circle, as can be seen in Fig. 3. This point represents the lowest received power P_{10} at the BS from the PMS, considering the detected location and ignoring other losses. Then, the radius of the secure forbidden region around the BS can be calculated as

$$r_s = (r_1 + u)\tau_p^{1/\alpha}. \tag{9}$$

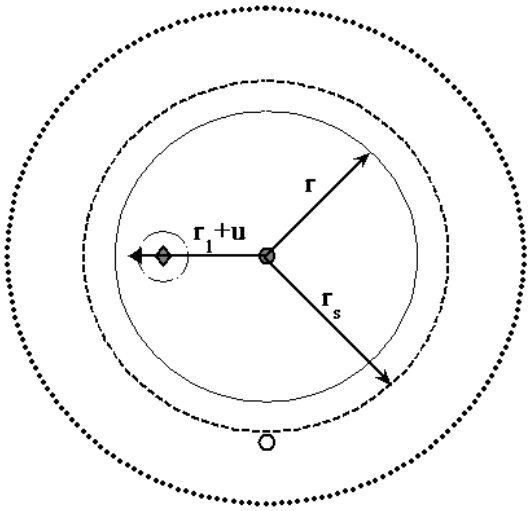

Fig. 3. Impact of location accuracy of the primary mobile station (PMS) on the forbidden region.

The area of the effective cognitive region, which guarantees the quality of the secondary link, varies in a more complex way because it depends on d_{12}, as well as on the actual position of the CRx, which is inside a small uncertainty circle centered at its original detected location as shown in Fig. 4.

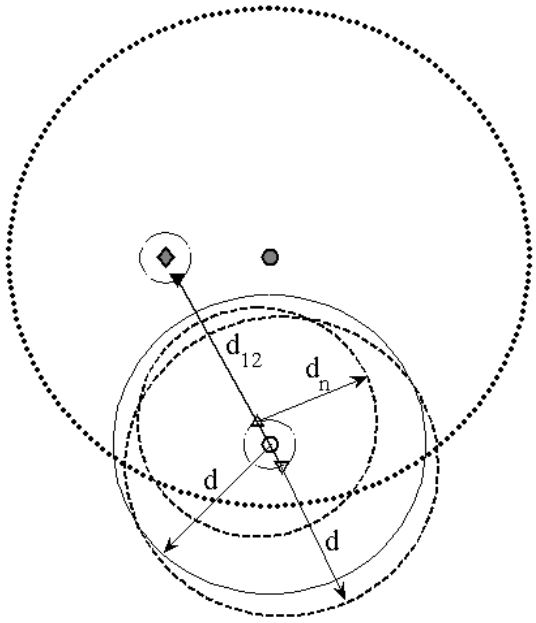

Fig. 4. Impact of location accuracy of the primary mobile station (PMS) and the cognitive receiver (CRx) on the effective cognitive region.

A simple analysis shows that when the PMS and the CRx are the closest to each other, see Fig. 4, the distance between the two devices determines the circumference of smallest possible radius $d_n = \frac{(d_{12}-2u)}{\tau_s^{1/\alpha}}$ centered at the assumed position of the CRx. However, having determined d_n, does not guarantee that all points contained in the circle of radius d_n are valid and not excluded by others with greater radius, as shown in Fig. 4. In addition, it should be considered another circle of radius d but centered at the farthest position from the PMS. It is necessary to find the secure effective cognitive region that is common to all possible effective cognitive regions regarding each detected location of the CRx. For a better understanding of this situation we resort to the illustration in Fig. 5.

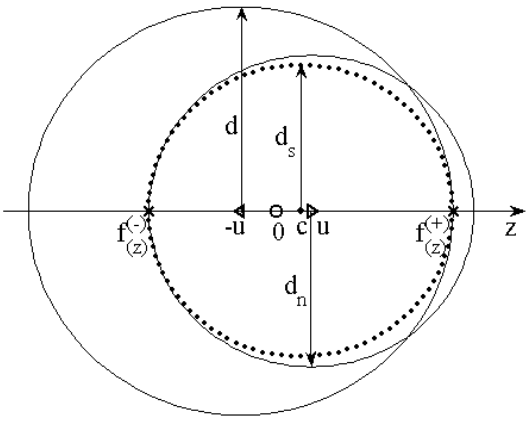

Fig. 5. Secure effective cognitive region.

The z-axis represents the straight line connecting the points (r_1,θ_1) and (r_2,θ_2), which represent the detected locations of the PMS and the CRx, respectively. The point (r_2,θ_2) is represented at $z=0$ in Fig. 5. Let the function $f_{(z)} = z \pm \frac{d_{12}-(u+z)}{\tau_s^{1/\alpha}}$ represent the intersection point between the z-axis and the circumference centered at some point in the interval $[-u,u]$, with radius equal to the second term of $f_{(z)}$. The plus sign in $f_{(z)}$ represents the constraint closest to the PMS and the minus sign in $f_{(z)}$ represents the constraint farthest from the PMS, which limits the maximum separation between the CTx and the CRx, for the worse cases. By evaluating this function we determine the positive cutoff $f_{(z)}^{(+)} = -u + \frac{d_{12}}{\tau_s^{1/\alpha}} = -u + d$ and the negative cutoff $f_{(z)}^{(-)} = -u - \frac{d_{12}-2u}{\tau_s^{1/\alpha}} = -u + d_n$. Now, the center c and radius d_s of the secure effective cognitive region can be determined as:

$$c = \frac{u}{\tau_s^{1/\alpha}}, \tag{10}$$

$$d_s = \frac{d_{12} - \left(u + \tau_s^{1/\alpha}\right)}{\tau_s^{1/\alpha}}. \tag{11}$$

Using r_s and d_s instead of r and d in (6), (7) and (8), it is possible to find the area of the secure concurrent transmission region, $\mathcal{R}_{CTS}$, which is shadowed in Fig. 6. The probability of being in this region can be computed as:

$$\mathcal{P}_{CTS} = \frac{\mathcal{R}_{CTS}}{\pi R^2}. \tag{12}$$

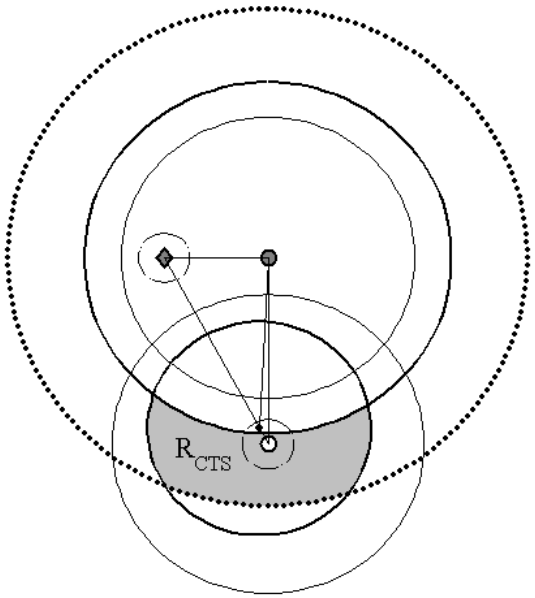

Fig. 6. Concurrent transmission region considering the detected positions as absolutely accurate. The PMS is located at $(40\,\text{m}, \pi)$ and the CRx is located at $\left(75\,\text{m}, \frac{3\pi}{2}\right)$.

It should be noted that in some sense this is a pessimistic approach because it prioritizes the primary link quality over the cognitive network performance. Any combination of real positions of the PMS and the CRx within their respective uncertainty areas, would allow to dimension a region such that $\mathcal{R}_{CT} > \mathcal{R}_{CTS}$. However, the secure concurrent transmission region is the only region that guarantees absolutely non-interference between links, regardless of real positions, only based on the detected positions and the uncertainty radius u. Now, knowing $\mathcal{P}_{CTS}$ it is possible to evaluate the suitability of reusing the frequency band inside the delimited region. However, how could one know whether a particular CTx satisfies the condition $(r_s < r_3 < R) \cap (d_{32s} < d_s)$?

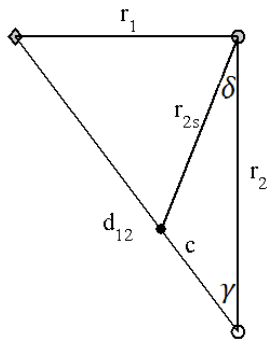

Fig. 7. New position of the CRx depending on u and the estimated locations of the PMS and the CRx.

In order to answer this question, we must know the distance between the CTx and the new position of the CRx, which is assumed to be at distance c from the origin in Fig. 5. For calculating this distance (d_{32s}), we need to find the coordinates (r_{2s}, θ_{2s}) of the new position of the CRx, which is represented by a black dot in Fig. 6. With the aid of Fig. 7, these coordinates can be computed as:

$$r_{2s} = \sqrt{r_2^2 + c^2 - 2r_2 c\cos(\gamma)}, \tag{13}$$

$$\theta_{2s} = \theta_2 + \vartheta. \tag{14}$$

The angle ϑ is measured from r_2 to r_{2s}, in counterclockwise direction. Note that in Figs. 6 and 7, $\vartheta = 2\pi - \delta$ which results in $\theta_{2s} = \theta_2 - \delta$. On the other hand, in settings where $\vartheta = \delta$, $\theta_{2s} = \theta_2 + \delta$. Note also that when the BS, the PMS and the CRx are located on the same line, as in Fig. 1, then $\gamma = 0$ and therefore (13) reduces to $r_{2s} = r_2 - c$, as expected. If necessary, these angles can be computed using the law of cosines as, $\gamma = \cos^{-1}\left(\frac{r_2^2 + d_{12}^2 - r_1^2}{2r_2 d_{12}}\right)$ and $\delta = \cos^{-1}\left(\frac{r_2^2 + r_{2s}^2 - c^2}{2r_2 r_{2s}}\right)$.

Another element should be considered: the location uncertainty range of the CTx. Having noticed that the CTx location is subject to the same uncertainty range that the CRx and the PMS, a condition to estimate its impact is to ensure that the CTx is always inside the secure concurrent transmission region for any location. This would imply that any detected location of CTx (r_3, θ_3) is at least at a distance u from any boundary of this region, that is, increasing r_s of u units, also causes a decrease in d_s and R of u units, ensuring that the CTx and its associated uncertainty region are inside the secure region. However, this is a very conservative approach for protecting the primary link which considerably reduces the $\mathcal{R}_{CTS}$. Simulation results allow us to confirm that even when the detected CTx location is at a breaking point of the delimited secure region, the mean probability of effectively being out of a concurrent transmission region is less than 3 %. Therefore, it is more important to protect the ad hoc network performance, keeping unchanged the $\mathcal{R}_{CTS}$, despite the uncertainty range of the CTx location.

4. Shadowing Effects

In the previous section, we only consider the impact of path loss on the concurrent transmission probability of a CR network overlaying a primary network. However, in real-world channels shadowing may be a major source of environment dependence in the measured RSS (Received Signal Strength). Due to shadowing, even though the CR device is located inside the secure concurrent transmission region, a peer-to-peer ad hoc connection may not be able to coexist with the primary infrastructured link.

Environment-dependent variations in RSS measurements due to shadowing may come from a large obstruction such as a furniture, a wall, a tree or a large building between the transmitter and receiver path. The shadowing effect can be modeled as a random processes (as a function of the environment in which the network is deployed) [56]. In particular, the difference between a measured received power and its ensemble average, due to random shadowing, is modeled

as a log-normal random process [56, 57], based on a wide variety of measurement results [55,58,59] and analytical evidences [60].

Let $10^{\varepsilon_{kj}/10}$ be the shadowing component in the propagation path between user $k \in \{1,3\}$ and user $j \in \{0,2\}$, where ε_{kj} is a sample of a Gaussian random variable with zero mean and standard deviation σ_ε. Then, the uplink signal-to-noise ratios in both the infrastructure-based link and the CR-based ad hoc link are rewritten as:

$$SIR_{p(\varepsilon_{10},\varepsilon_{30})} = \frac{10^{\varepsilon_{10}/10}/r_{1s}^{\alpha}}{10^{\varepsilon_{30}/10}/r_{3}^{\alpha}}, \tag{15}$$

$$SIR_{s(\varepsilon_{32},\varepsilon_{12})} = \frac{10^{\varepsilon_{32}/10}/d_{32s}^{\alpha}}{10^{\varepsilon_{12}/10}/d_{12s}^{\alpha}}. \tag{16}$$

Taking into account the shadowing effect, the secure concurrent transmission probability can be expressed as:

$$\mathcal{P}_{CTS}(\varepsilon) = \left\{ \left(r_s 10^{(\varepsilon_{30}-\varepsilon_{10})/10\alpha} < r_3 < R \right) \cap \left(d_{32s} < d_s 10^{(\varepsilon_{32}-\varepsilon_{12})/10\alpha} \right) \right\}. \tag{17}$$

We define the reliability of uplink secure concurrent transmission, $\mathcal{F}_{CTS}(\varepsilon)$, as the probability that, given that the CTx is in the region $\mathcal{R}_{CTS}$, a CR device can successfully establish an ad hoc link in the presence of the primary user uplink transmission subject to the shadowing effect:

$$\mathcal{F}_{CTS}(\varepsilon) = \mathcal{P}\left\{ (SIR_{p(\varepsilon_p)} > \tau_p) \cap (SIR_{s(\varepsilon_a)} > \tau_s) | \text{CTx} \in \mathcal{R}_{CTS} \right\}. \tag{18}$$

Note that $\mathcal{F}_{CTS}(\varepsilon) = 1$ when shadowing is not considered. Assume that ε_{kj} have the same standard deviation for all k and j and let $\varepsilon_p = \varepsilon_{30} - \varepsilon_{10}$ and $\varepsilon_a = \varepsilon_{32} - \varepsilon_{12}$. Then, ε_p and ε_a become samples of Gaussian random variables with zero mean and standard deviation $\sqrt{2}\sigma_\varepsilon$. In this case, it is most useful to analyze the effect of shadowing by simulation, as we do next.

5. Numerical Results

From the topology shown in Fig. 1 with $R = 100$ m, $N = 10^6$ points were uniformly distributed in a region with area equal to πR^2, representing possible locations of the CTx. In addition, $n = 10^3$ uniformly distributed points representing possible real combination of PMS and CRx locations were generated within its respective uncertainty circles centered at the detected coordinates $\left(25, \frac{\pi}{2}\right)$ and $\left(50, \frac{3\pi}{2}\right)$. The values considered for the radius of the uncertainty circles were $u = 0, 1, 3, 5, 10$ and 15 m. Moreover, we assume $\alpha = 4$, $\tau_p = 8.45$ dB and $\tau_s = 0$ dB. The simulation results are compared to $\mathcal{P}_{CTS}$, estimated from the presented analytical model.

Figure 8 shows the impact of location uncertainty on the concurrent transmission probability. The curve labeled "Ideal P_{CT}" is the concurrent transmission probability when considering a positioning system with perfect accuracy, as in [25]. The "Analytical P_{CTS}" curve is obtained from the novel analytical model, while the numerical result is labeled as "Simulated P_{CTS}". From Fig. 8 it can be seen that the simulated and analytical results match very well, showing the rapid decrease of $\mathcal{P}_{CTS}$ with the increase in u. Moreover, note that the idealized analysis in [25], which does not consider the location uncertainty, is considerably optimistic.

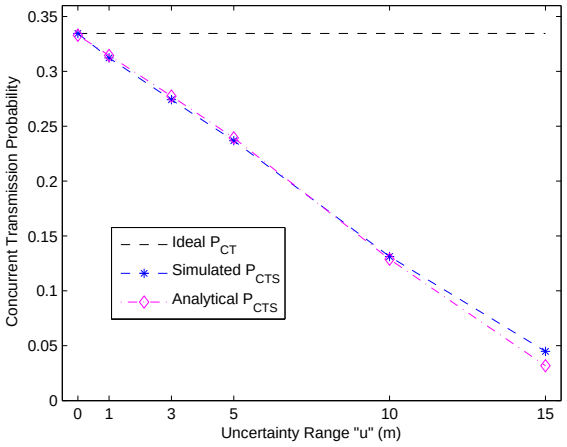

Fig. 8. Concurrent transmission probability as a function of the uncertainty range.

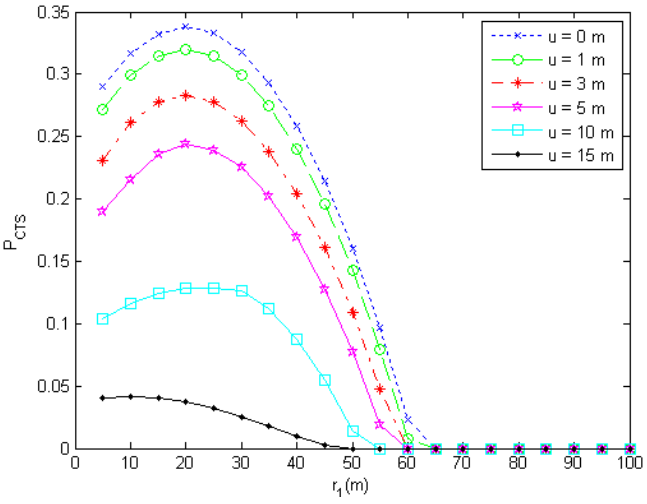

Fig. 9. Secure concurrent transmission probability as a function of the distance from the PMS to the BS, considering $r_2 = 50$ m.

Figure 9 shows the impact of the uncertainty range on the secure concurrent transmission probability when r_1 is varied, with $r_2 = 50$ m and the values of θ_1 and θ_2 are kept constant. Note how the secure concurrent transmission probability decreases when u is increased, for the same value of r_1, since r_s increases to protect the primary link according to (9) and d_s decreases to protect the secondary link according to (11). It must be also noted that increasing u reduces the

maximum allowable value for r_1 which satisfies $\mathcal{P}_{CTS} \neq 0$. From (9) it can be noted that the protection radius (r_s) for the primary link is increased with r when $u = 0$ in $u\tau_p^{1/\alpha}$, thus $r_s = R$ for $r_1 = 61.48, 60.48, 58.48, 56.48, 51.48$ and 46.48 for $u = 0, 1, 3, 5, 10$ and 15 m, respectively. The figure illustrates that it is favorable to decrease r_1, since the received signal at the BS from the PMS is stronger, decreasing the probability of interference, and thus, reducing the size of the forbidden region. Note that the maximum value of $\mathcal{P}_{CTS}$ is not reached by the lowest value of r_1 because, while the PMS is approaching the BS, it also becomes closer to the CRx, and thus it may affect the secondary link.

Figure 10 shows the impact of the uncertainty range when r_2 is varied, while $r_1 = 25$ m and θ_1 and θ_2 are kept constant. The secure concurrent transmission probability also decreases when u is increased, for the same value of r_2, since d_s is decreased to protect the secondary link according to (11). Note now that the favorable trend is the increase in r_2 closer to R, since d_{12} increases and this implies the increase of d_s according to (11), because the received power at the CRx from the PMS decreases and, therefore, the probability of the secondary link being interfered also decreases. The minimum values of r_2 that satisfy $\mathcal{P}_{CTS} \neq 0$ depend on fulfilling the condition $r_s < r_{2s} + d_s$, as explained above, and are given by $r_2 = 7.9, 10.2, 14.8, 19.4, 31.0$ and 42.6 for $u = 0, 1, 3, 5, 10$ and 15 m, respectively.

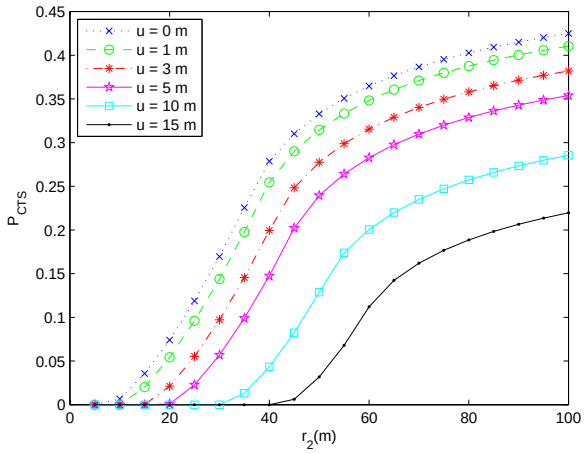

Fig. 10. Secure concurrent transmission probability as a function of the distance from the CRx to the BS, considering $r_1 = 25$ m.

From the analytical model, the coordinates of the PMS and CRx associated with the maximum value of $\mathcal{P}_{CTS}$ when $u = 0$ can be determined, which are $\left(20, \frac{\pi}{2}\right)$ and $\left(100, \frac{3\pi}{2}\right)$, respectively. Figure 11 shows combinations of these coordinates with the coordinates $\left(50, \frac{\pi}{2}\right)$ and $\left(50, \frac{3\pi}{2}\right)$, to show the relationship between $\mathcal{P}_{CTS}$ and u for different arrangements of the mobile stations involved in the scenario.

In Fig. 11, the upper curve shows an apparent promising behavior regarding the increase in u, taking into account that for an uncertainty range of 27 m (equivalent to 27 % of coverage radius) the concurrent transmission probability is still higher than 0.1. However, note how increasing r_1 or decreasing r_2, until 50 m, causes a significant decrease on $\mathcal{P}_{CTS}$. For example, when $u = 5$ m, the red curve shows a value close to 65 % of the optimal curve (blue curve), the green curve shows a value close to 28 % and the black curve shows a value close to 21 %. If a concurrent transmission region with area greater than 25 % of the coverage area of the BS is desired, an uncertainty range greater than 5 m hinders the fulfillment of this criterion, when $r_1 > 50$ m and/or $r_2 < 50$ m. If a uniform distribution is considered in the coverage area, the previous conditions represent more than 80 % of the cases.

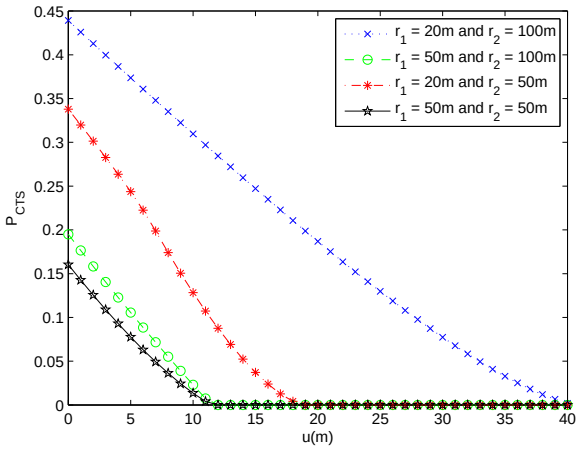

Fig. 11. Secure concurrent transmission probability as a function of the uncertainty range for different topologies

In order to quantify the effect of using our proposal instead of the method in [25], we estimate the percentage of *false positives* – when opportunities for concurrent transmission are erroneously identified based on the estimated location of the devices, which cause harmful interference at some links; as well as the percentage of *false negatives* – when it is decided not to concurrently transmit but, given the actual locations of the devices, the transmission could be performed without interfering any links. Table 1 shows the proportion of false negatives and false positives considering two different scenarios: A) $r_1 = 20$ m and $r_2 = 100$ m and B) $r_1 = 50$ m and $r_2 = 50$ m. In the table FN (FP) represents the proportion of false negatives (false positives) when the model of [25] is used while FN-U (FP-U) is the proportion of false negatives (false positives) when the method proposed in this paper is used so that location uncertainty is taken into account. Note that the amount of false negatives increases with the use of the proposed scheme (FN-U is larger than FN), so that some concurrent transmission opportunities are actually missed. However, such conservative approach has a quite beneficial consequence, that is to bring the number of false positives (FP-U) very close to zero. This means that with the use of the proposed scheme the secondary users almost never suffer

from interference and they in turn will never interfere with the primary users, something that cannot be guaranteed with the method in [25]. That is the main difference between the use of the method in [25] or the one proposed in this work: the primary link is protected even in the presence of location uncertainty.

	u (m)	1	3	5	10	15
	FN-U (%)	2.3	6.5	10.1	17.4	22.7
A	FN (%)	0.5	1.4	2.2	3.8	5.0
	FP-U (%)	0.0016	0.0050	0.0083	0.0162	0.0218
	FP (%)	0.6	1.9	3.4	7.0	11.1
	FN-U (%)	2.0	5.7	8.7	13.9	14.3
B	FN (%)	0.4	1.3	2.0	3.6	4.8
	FP-U (%)	0.0017	0.0047	0.0058	0.0030	—
	FP (%)	2.3	7.1	11.8	24.2	35.7

Tab. 1. False negatives and false positives considering the method in [25] (FN and FP) and the method proposed in this paper (FN-U and FP-U) that accounts for location uncertainty.

The reliability of the concurrent transmission, taking into account the effect of shadowing, was estimated by simulation. In addition to the parameters described at the beginning of this section, here we assume $\sigma_\varepsilon = 1, 3, 5$ and 10 dB. For each established link we consider $m = 10^3$ normally distributed values for ε_{kj} with zero mean and standard deviation σ_ε, in order to consider the shadowing effect. The PMS and the CRx are considered to be located at $\left(25, \frac{\pi}{2}\right)$ and $\left(50, \frac{3\pi}{2}\right)$, respectively.

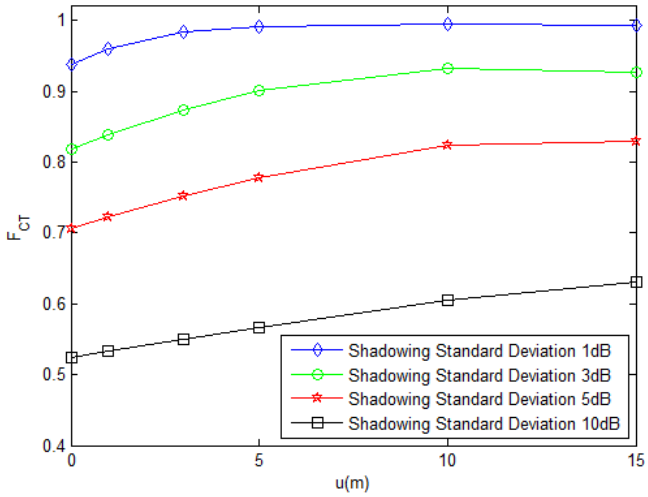

Fig. 12. Reliability of uplink secure concurrent transmission as a function of the uncertainty range, considering $r_1 = 25$ m and $r_2 = 50$ m

Figure 12 shows an apparent contradiction between the reliability of uplink secure concurrent transmission and the uncertainty range of the locations, since this reliability increases when u is increased. However, this result is consistent with the decrease in the secure concurrent transmission region when the uncertainty range increases, because interference between both links is less likely to occur when the CTx is within a region whose area decreases when increasing u. Note that, in general, the larger shadowing variance leads to a lower reliability for uplink concurrent transmissions. For example when u is in the range $1 \sim 15$ m, $\mathcal{F}_{CTS}(\varepsilon)$ is larger than 0.93 for $\sigma_\varepsilon = 1$ dB whereas it decreases to $0.52 \sim 0.64$ for $\sigma_\varepsilon = 10$ dB.

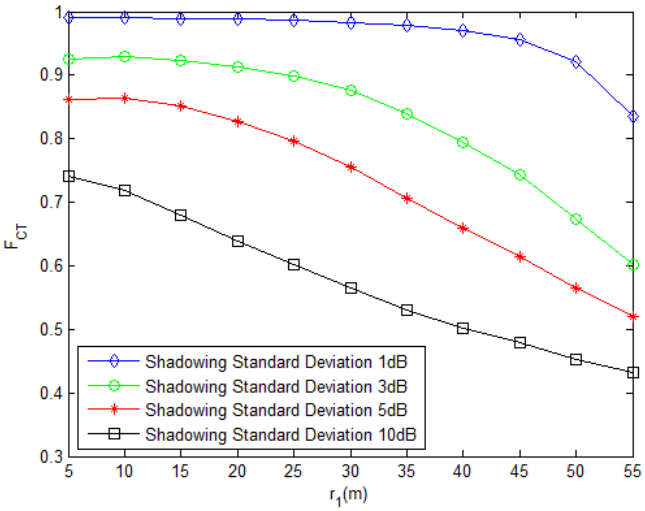

Fig. 13. Reliability of uplink secure concurrent transmission as a function of the distance from the PMS to the BS, considering $r_2 = 50$ m and $u = 5$ m.

Figures 13 and 14 illustrate the reliability of the secure concurrent transmissions with various shadowing standard deviation values versus r_1 and r_2, respectively.

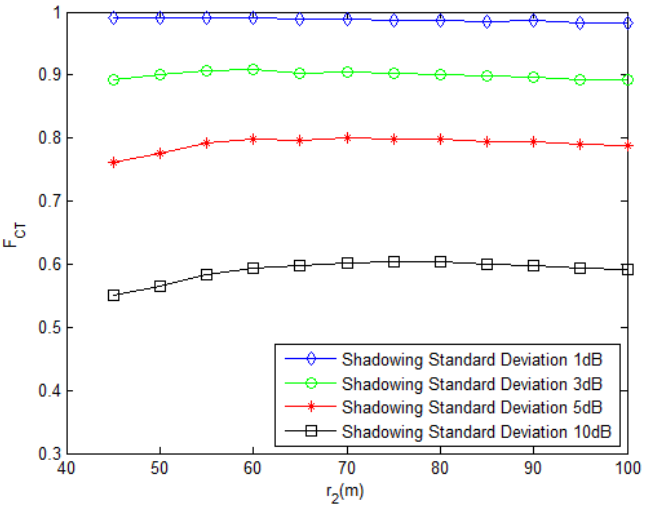

Fig. 14. Reliability of concurrent transmission as a function of the distance from the CRx to the BS, considering $r_1 = 25$ m and $u = 5$ m.

In Fig. 13, when r_1 is in the range $5 \sim 55$ m, $\mathcal{F}_{CTS}(\varepsilon)$ is larger than 0.83 for $\sigma_\varepsilon = 1$ dB whereas it decreases to $0.75 \sim 0.43$ for $\sigma_\varepsilon = 10$ dB. It should be noted that, when the primary user moves away from the BS, the reliability

of concurrent transmissions decreases due to shadowing and weaker RSS; for $\sigma_\varepsilon = 3$ dB $\mathcal{F}_{CTS}(\varepsilon)$ decreases from 0.93 to 0.6. In Fig. 14, it is shown that, subject to the influence of shadowing, the reliability of uplink secure concurrent transmission increases when the receiver of the ad hoc link approaches the cell edge. Clearly, the interference from the primary user to the ad hoc link becomes weaker when the ad hoc users move away from the BS. Again, the larger shadowing variance leads to a lower reliability for uplink concurrent transmission; when r_2 is in the range $45 \sim 100$ m, $\mathcal{F}_{CTS}(\varepsilon)$ is larger than 0.98 for $\sigma_\varepsilon = 1$ dB whereas it decreases to $0.55 \sim 0.6$ when $\sigma_\varepsilon = 10$ dB.

6. Conclusions

A new analytical model to identify a secure concurrent transmission region is proposed, which guarantees the coexistence of primary and secondary links in location-aware cognitive radio networks, taking into account the uncertainty associated with the locations of the mobile devices obtained from conventional positioning systems. In addition, the proposed analytical model allows to assess and decide about the convenience of selecting and reusing a specific frequency band depending on the location of the mobile devices and the positioning accuracy. The results show the importance of using positioning techniques and algorithms of high accuracy in order to achieve high throughput and efficient spectrum reuse. From these results, we may confidently conclude that position uncertainties above 5 m prevent achieving a secure concurrent transmission probability greater than 0.25, for more than 80 % of the cases considered in the topology under study. Also, an analytical method to determine the lower boundary for the reliability of the predetermined concurrent transmission region under shadowing effects was proposed, showing how the uncertainty range significantly affects the reliability. As future research works we plan: i) to consider the case where, for each device, the uncertainty radius is a function of the particular node location, which should be a more precise and much less pessimistic approach; ii) to analyze the use of power control as a mechanism to cope with the decline in concurrent transmission probability when the location uncertainty increases.

Acknowledgements

This work was partially supported by CAPES (Brazil).

References

[1] WANG, B., LIU, K. J. R. Advances in cognitive radio networks: A survey. *IEEE Journal of Selected Topics in Signal Processing*, 2011, vol. 5, no. 1, p. 5 - 23.

[2] ZENG, B., LIANG, Y. C., HOANG, A. T., ZHANG, R. A review on spectrum sensing for cognitive radio: Challenges and solutions. *EURASIP Journal on Advances in Signal Processing*, 2011, p. 1 - 16.

[3] Federal Communications Commission. *Report of the Spectrum Efficiency Working Group*. Spectrum Policy Task Force, 2010.

[4] ISLAM, H., KOH, C. L., OH, S. W., QING, X., LAI, Y. Y., et al. Spectrum survey in Singapore: Occupancy measurements and analyses. In *Proceedings of 3rd International Conference on Cognitive Radio Oriented Wireless Networks and Communications*. Singapore, 2008, p. 1 - 7.

[5] McHENRY, M. Spectrum white space measurements. In *New America Foundation Broadband Forum*. 2008, p. 1 - 13.

[6] Federal Communications Commission. *Notice of Proposed Rule Making and Order: Facilitating Opportunities for Flexible, Efficient, and Reliable Spectrum use Employing Cognitive Radio Technologies*. ET Docket No. 03–108, 2003.

[7] MITOLA, J., MAGUIRE, G. Q. Cognitive radio: making software radios more personal. *IEEE Personal Communications*, 1999, vol. 6, no. 4, p. 13 - 18.

[8] HAYKIN, S. Cognitive radio: Brain-empowered wireless communications. *IEEE Journal on Selected Areas in Communications*, 2005, vol. 23, p. 201 - 220.

[9] AKYILDIZ, I., LEE, W., VURAN, M., MOHANTY, S. NeXt generation/dynamic spectrum access/cognitive radio wireless networks: A survey. *Computer Networks*, 2006, vol. 50, p. 2127 - 2159.

[10] MARINHO, J., MONTEIRO, E. Cognitive radio: Survey on communication protocols, spectrum decision issues, and future research directions. *Wireless Networks*, 2012, vol. 18, no. 2, p. 147 - 164.

[11] Federal Communications Commission. *In the Matter of Unlicensed Operation in the TV Broadcast Bands Additional Spectrum for Unlicensed Devices Below 900 MHz and in the 3 GHz Band*. ET Docket 08 - 260, 2009.

[12] YUCEK, T., ARSLAN, H. A survey of spectrum sensing algorithms for cognitive radio applications. *IEEE Communications Surveys & Tutorials*, 2009, vol. 11, pp. 116 - 130.

[13] CABRIC, D., MISHRA, S. M., BRODERSEN, R. W. Implementation issues in spectrum sensing for cognitive radios. In *Conference Record of the 38th Asilomar Conference on Signals, Systems and Computers*. 2009, p. 772 - 776.

[14] ZHANG, Z., WU, Q., WANG, J. Energy-efficient power allocation strategy in cognitive relay networks. *Radioengineering*, 2012, vol. 21, no. 3, p. 809 - 814.

[15] NOURI, N., NOORI, N. Directional relays for multi-hop cooperative cognitive radio networks. *Radioengineering*, 2013, vol. 22, no. 3, p. 791 - 799.

[16] FATHI, H., SADOUGH, S. Robust power and subcarrier allocation for OFDM-based cognitive radio networks considering spectrum sensing uncertainties. *Radioengineering*, 2013, vol. 22, no. 3, p. 810 - 817.

[17] SONG, Y., XIE, J. Optimal power control for concurrent transmissions of location-aware mobile cognitive radio ad hoc networks. In *Proceedings of the IEEE Global Telecommunications Conference*. Honolulu (USA), 2009, pp. 1 - 6.

[18] ZHAO, Q., TONG, L., SWAMI, A. A cross-layer approach to cognitive MAC for spectrum agility. In *Conference Record of the Thirty-Ninth Asilomar Conference on Signals, Systems and Computers*. Pacific Grove (CA, USA), 2005, p. 200 - 204.

[19] CELEBI, H., ARSLAN, H. Utilization of location information in cognitive wireless networks. *IEEE Wireless Communications*, 2007, vol. 14, no. 4, p. 6 - 13.

[20] KÜHN, P. Location-based services in mobile communication infrastructures. *AEU - International Journal of Electronics and Communications*, 2004, vol. 58, no. 3, p. 159 - 164.

[21] GEZICI, S. A survey on wireless position estimation. *Wireless Personal Communications*, 2008, vol. 44, p. 263 - 282.

[22] GORCIN, A. RSS-based location awareness for public safety cognitive radio. In *Proceedings of 1st International Conference on Wireless Communication, Vehicular Technology, Information Theory and Aerospace & Electronic Systems Technology*. Aalborg (Denmark), 2009, p. 520 - 524.

[23] GURNEY, D., BUCHWALD, G., ECKLUND, L., KUFFNER, S. L., GROSSPIETSCH, J. Geo-location database techniques for incumbent protection in the TV white space. In *Proceedings of 3rd IEEE Symposium on New Frontiers in Dynamic Spectrum Access Networks*. Chicago (IL, USA), 2008, p. 1 - 9.

[24] SHELLHAMMER, S. J. A comparison of geo-location and spectrum sensing in cognitive radio. In *Proceedings of the 18th International Conference on Computer Communications and Networks*. San Francisco (CA, USA), 2009, p. 1 - 6.

[25] WANG, L.-C., CHEN, A. Effects of location awareness on concurrent transmissions for cognitive ad hoc networks overlaying infrastructure-based systems. *IEEE Transactions on Mobile Computing*, 2009, vol. 8, p. 577 - 589.

[26] JALAEIAN, B., MOTANI, M. Location aware CR-MAC: A multichannel cross layered PHY-MAC protocol for cognitive radio ad hoc networks. In *Proceedings of IEEE 9th Malaysia International Conference on Communications*. Kuala Lumpur (Malaysia), 2009, p. 348 - 353.

[27] MONTEJO-SANCHEZ, S., SOUZA, R. D., FERNANDEZ, E. M. G., ALFONSO-REGUERA, V. Impact of rate control on the performance of a cognitive radio ad-hoc network. *IEEE Communications Letters*, 2012, vol. 16, no. 9, p. 1424 - 1427.

[28] MONTEJO-SANCHEZ, S., FERNANDEZ, E. M. G., ALFONSO-REGUERA, V., GODOY, W. Power control and concurrent transmission for cognitive ad hoc networks. *IEEE Latin America Transactions*, 2013, vol. 11, no. 2, p. 857 - 864.

[29] MONTEJO-SANCHEZ, S., SOUZA, R. D., FERNANDEZ, E. M. G., ALFONSO-REGUERA, V. Rate and energy efficient power control in a cognitive radio ad hoc network. *IEEE Signal Processing Letters*, 2013, vol. 20, no. 5, p. 451 - 454.

[30] HASSAN, D. M. R., KARMAKAR, G., KAMRUZZAMAN, J. Maximizing the concurrent transmissions in cognitive radio ad hoc networks. In *Proceedings of the 7th International Wireless Communications and Mobile Computing Conference*. Istanbul (Turkey), 2011, p. 466 - 471.

[31] MONTEJO-SANCHEZ, S., SOUZA, R. D., FERNANDEZ, E. M. G., ALFONSO-REGUERA, V. Impact of power allocation and antenna directivity in the capacity of a multiuser cognitive ad hoc network. *Radioengineering*, 2012, vol. 21, no. 4, p. 1110 - 1116.

[32] LIN, Y., HSU, Y. Multihop cellular: A new architecture for wireless communications. In *Proceedings of IEEE INFOCOM*. Tel Aviv (Israel), 2000, vol. 3, p. 1273 - 1282.

[33] WU, H., QIAO, C., DE, S., TONGUZ, O. Integrated cellular and ad hoc relaying systems: iCAR. *IEEE Journal on Selected Areas in Communications*, 2001, vol. 19, no. 10, p. 2105 - 2115.

[34] WU, E. H. K., HUANG, Y. Z., CHIANG, J. H. (2001). Dynamic adaptive routing for heterogeneous wireless network. In *Proceedings of IEEE Global Telecommunications Conference GLOBECOM*. San Antonio (TX, USA), 2001, vol. 6, p. 3608 - 3612.

[35] YANMAZ, E., TONGUZ, O. K., MISHRA, S. Efficient dynamic load balancing algorithms using iCAR systems: a generalized framework. In *Proceedings of IEEE 56th Vehicular Technology Conference VTC 2002 - Fall*. Vancouver (Canada), 2002, p. 586 - 590.

[36] CHENG, J., CHAN, S. H. G., HE, J., LIEW, S. Mixed-mode WLAN: the integration of ad hoc mode with wireless LAN infrastructure. In *Proceedings of IEEE Global Telecommunications Conference GLOBECOM*. San Francisco (USA), 2003, p. 231 - 235.

[37] AL-KHASIB, T., LAMPE, L. Admission control and resource optimization for multiple-user OFDMA cognitive radio systems. *AEU - International Journal of Electronics and Communications*, 2012, vol. 66, no. 5, p. 401 - 409.

[38] CELEBI, H., ARSLAN, H. Adaptive positioning systems for cognitive radios. In *Proceedings of 2nd IEEE International Symposium on New Frontiers in Dynamic Spectrum Access Networks*. Dublin (Ireland), 2007, p. 78 - 84.

[39] CELEBI, H., ARSLAN, H. Cognitive positioning systems. *IEEE Transactions on Wireless Communications*, 2007, vol. 6, no. 12, p. 4475 - 4483.

[40] CELEBI, H., ARSLAN, H. Enabling location and environment awareness in cognitive radios. *Computer Communications*, 2008, vol. 31, p. 1114 - 1125.

[41] HIGHTOWER, J., BORRIELLO, G. Location systems for ubiquitous computing. *Computer*, 2001, vol. 34, no. 8, p. 57 - 66.

[42] NICULESCU D., NATH, B. Ad hoc positioning system (APS). In *Proceedings of the IEEE Global Telecommunications Conference*. San Antonio (USA), 2001, p. 2926 - 2931.

[43] NICULESCU, D. Ad hoc positioning system (APS) using AOA. *Proceedings of IEEE INFOCOM*. San Francisco (USA), 2003, vol. 3, p. 1734 - 1743.

[44] CELEBI, H., QARAQE, K. A., ARSLAN, H. Performance analysis of TOA range accuracy adaptation for cognitive radio systems. In *Proceedings of IEEE 70th Vehicular Technology Conference - VTC Fall*. Anchorage (USA), 2009, p. 1 - 4.

[45] CHAFFEE, J., ABEL, J. GDOP and the Cramér-Rao bound. In *Proceedings of IEEE Position Location and Navigation Symposium*. Las Vegas (NV, USA), 1994, p. 663 - 668.

[46] SAYED, A. H., TARIGHAT, A., KHAJEHNOURI, N. Network-based wireless location: Challenges faced in developing techniques for accurate wireless location information. *IEEE Signal Processing Magazine*, 2005, vol. 22, no. 4, p. 24 - 40.

[47] MONTEJO-SANCHEZ, S., ALFONSO-REGUERA, V., FERNANDEZ, E. M. G., GODOY, W. Impact of location accuracy on concurrent transmission for cognitive ad hoc networks. In *Proceedings of the 2011 IEEE Latin-American Conference on Communications (LATINCOM)*. Belém (Brazil), 2011, p. 1 - 6.

[48] MADIGAN, D., EINAHRAWY, E., MARTIN, R. P., JU, W.-H., KRISHNAN, P., KRISHNAKUMAR, A. S. Bayesian indoor positioning systems. In *Proceedings of IEEE 24th Annual Joint Conference of the IEEE Comp and Comm Societies INFOCOM*. Miami (USA), 2005, vol. 2, p. 1217 - 1227.

[49] GOULIN, K. J. R., CHEN, J., GUO, W., LIU. Signal Processing techniques in network-aided positioning: A survey of state-of-the-art positioning designs. *IEEE Signal Processing Magazine*, 2005, vol. 22, no. 4, p. 12 - 23.

[50] TSENG, Y., WU, S., LIAO, W., CHAO, C. Location awareness in ad hoc wireless mobile networks. *Computer*, 2001, vol. 34, no. 6, p. 46 - 52.

[51] MAUVE, M., WIDMER, A., HARTENSTEIN, H. A survey on position-based routing in mobile ad hoc networks. *IEEE Network*, 2001, vol. 15, no. 6, p. 30 - 39.

[52] HONG, X., XU, K., GERLA, M. Scalable routing protocols for mobile ad hoc networks. *IEEE Network*, 2002, vol. 16, no. 4, p. 11 - 21.

[53] AL-KARAKI, J. N., KAMAL, A. E. Routing techniques in wireless sensor networks: A survey. *IEEE Wireless Communications*, 2004, vol. 11, p. 6 - 28.

[54] HOU, Y. T., REED, J. H. Exploiting location information for concurrent transmissions in multihop wireless networks. *IEEE Transactions on Vehicular Technology*, 2009, vol. 58, p. 314 - 323.

[55] RAPPAPORT, T. S. *Wireless Communications: Principle and Practice*. 2nd ed. Prentice Hall, 2002.

[56] PATWARI, N., ASH, J. N., KYPEROUNTAS, S., HERO, O., MOSES, R. L., CORREAL, N. S. Locating the nodes: cooperative localization in wireless sensor networks. *IEEE Signal Processing Magazine*, 2005, vol. 22, p. 54 - 69.

[57] STÜBER, G. L. *Principles of Mobile Communication*. Springer, 2002.

[58] PATWARI, N., HERO, A. O., PERKINS, M., CORREAL, N. S., DEA, R. J. O. Relative location estimation in wireless sensor networks. *IEEE Transactions on Signal Processing*, 2003, vol. 51, p. 2137 - 2148.

[59] PATWARI, N., O'DEA, R. J., WANG, Y. Relative location in wireless networks. In *Proceedings of IEEE 53rd Vehicular Technology Conference VTC Spring*. Rhodes (Greece), 2001, vol. 2, p. 1149 - 1153.

[60] COULSON, A. J., WILLIAMSON, A. G., VAUGHAN, R. G. A statistical basis for lognormal shadowing effects in multipath fading channels. *IEEE Transactions on Communications*, 1998, vol. 46, no. 4, p. 494 - 502.

About Authors ...

Samuel MONTEJO was born in Camagüey, Cuba, in 1979. He received his M.Sc. degree in Telecommunications Engineering from Central University of Las Villas (UCLV), Cuba, in 2007. He is currently an assistant professor and a doctoral student at the Department of Telecommunications, UCLV. His research interests include localization algorithms, cognitive radio systems and wireless networks.

Richard D. SOUZA was born in Florianópolis, Brazil, in 1978. He received the B.Sc. and the D.Sc. degrees in Electrical Engineering from the Federal University of Santa Catarina (UFSC), Florianópolis, Brazil, in 1999 and 2003, respectively. From March 2003 to November 2003 he was a Visiting Researcher in the Department of Electrical and Computer Engineering at the University of Delaware, USA. Since April 2004 he has been with the Federal University of Technology - Paraná (UTFPR), Curitiba, Brazil, where he is now an Associate Professor. His research interests are in the area of error control coding and wireless communications.

Evelio M. G. FERNANDEZ was born in Santa Clara, Cuba, in 1962. He received his M.Sc. and Ph.D. degrees in electrical engineering from the State University of Campinas, Brazil in 1997 and 2001 respectively. He is currently an associate professor at the Department of Electrical Engineering at the Federal University of Paraná. His research interests include channel coding techniques, digital communications, wireless networks and cognitive radio systems.

Vitalio ALFONSO was born in Santa Clara, Cuba, in 1972. He received his M.Sc. degree in Telecommunications Engineering and his Ph.D. degree in Electrical Engineering from the Central University of Las Villas (UCLV), Cuba, in 2000 and 2007, respectively. He is currently an associate professor at the Department of Telecommunications, UCLV. His current research interests include cognitive radio, communication protocols, quality of service and wireless networks.

Walter GODOY was born in Araçatuba, São Paulo, Brazil, in 1950. He received the M.Sc. degree in Electrical Engineering from the Institute of Communications Engineering, St. Petersburg, Russia and the Ph.D. degree in Electrical Engineering from the State University of Campinas, Brazil, in 1977 and 1990, respectively. He is currently a Senior Professor at the Department of Electronics, Federal University of Technology - Paraná (UTFPR), Curitiba, Brazil. His main fields of research are Error-control Codes and their applications and Cryptography.